3. **Kubota N., Sonobe T., Yamamoto A. et al.** Burning rate characteristics of GAP propellants // J. Propulsion and Power.— 1990.— 6.— P. 686—689.
4. **Mishra I. B., Bickenbaugh D. E., Ashmore C. I. et al.** Development of GAP — TAGN — PEG propellant: JANNAF Propulsion meeting.— 1984.— 11.— P. 153—182.
5. **Kubota N., and Sonobe T.** Combustion of Mechanism of Azide Polymer: TRDL Tech. Report., RPL, June 1988.
6. **Farber M., Harris S. P., Shrivastava B. D.** Mass spectrometric kinetic studies of several azido polymers // Combust. Flame.— 1989.— 55.— P. 203.
7. **Oyumi Y. and Brill T. B.** Thermal decomposition of energetic materials. 12. Infrared spectral and rapid thermolysis studies of azide containing monomers and polymers // Ibid.— 1976.— 65.— P. 127—135.
8. **Mishra I. B., Juneau G. P., Groom T.** Combustion of GAP: JANNAF Propulsion Meeting.— 1984.— 11.— P. 7—9.
9. **Leu A. L. and Shen S. M.** Thermal characterisitics of GAP, GAP/BDNPA/BDNPF, PEG/BDNPA/BDNPF and the energetics composites thereof: 21st ICT, Jahrestag, Karlsruhe, Germany, 1990, 6/1—6/13.
10. **Nazare A. N., Asthana S. N., Singh, Haridwar.** GAP-an energetic component of advanced solid propellants // J. Energetic Materials (accepted for publication — 1992).
11. **Dhar S. S., Asthana S. N., Shrotri P. G. et al.** Pyrolysis/Combustion behaviour of GAP based double base propellants: 22nd ICT, Jahrestag, Karlsruhe, Germany. 1991, 58/1—58/7.
12. **Liu Z. B., Yiu C. M., Wu C. Y. et al.** The characteristic temperature method to estimate kinetic parameters from DTA curves and to evaluate the compatibility of explosives // Propellants, Explosives and Pyrotechnics.— 1986.— 11.— P. 11—15.
13. **Reich L.** Compatibility of polymer oil — highly energetic materials by DTA // Thermochimica Acta.— 1973.— 5.— P. 433.
14. **Maycock J. M.** Thermal analysis of explosives and solid propellants // Ibid.— 1970.— 1.— P. 387—407.
15. **Kissinger H. E.** // J. Res. Nat. Bur. Stand.— 1956.— 57.— P. 27.
16. **Ozawa T.** // J. Thermal Anal.— 1976.— 9.— P. 217.
17. **Coats A. W., and Bedfern J. P.** Kinetic parameters from TG data // Nature 201, 68 (1964).
18. **Ahad E.** Direct conversion of ECH to GAP polymer, US Patent 059,524.
19. **Bhat V. K., Singh, Haridwar et al.** Processing of high energy crosslinked composite modified double base propellants: 18th Jahrestag Frauhofer Inst. Treib Explosivst. Kalrsruhe, 1987, 18/1—18/10.

УДК 662.741.334

S. F. Son and M. Q. Brewster

UNSTEADY COMBUSTION OF SOLID PROPELLANTS SUBJECT TO DYNAMIC EXTERNAL RADIANT HEATING

Department of Mechanical and Industrial Engineering
University of Illinois at Urbana — Champaign

Abstract

A theoretical and experimental investigation is being conducted on the effect of a dynamic external radiant heat flux on the combustion of energetic materials. These studies have illustrated the need for including the effect of the mean radiant heat flux and in-depth absorption. Also, a method for obtaining the linear frequency response function over a range of frequencies from a single test using series of radiant pulses is demonstrated. Experimental results have been obtained for an AP/HTPB propellant.

Introduction

There is a growing recognition of the advantages of studying the combustion of energetic solids, particularly solid propellants, using unsteady external radiant energy sources such as lasers. A reason this particular approach has recently received renewed interest is that it is easier to control a radiant flux and to simultaneously measure the instantaneous burning rate than to perform a similar experiment with an unsteady pressure field. The purpose of this paper is to illustrate the effect of primary parameters based on QSHOD (quasi-steady gas and surface reaction, homogeneous propellant, and one-dimensional flame) analysis of radiant flux driven combustion and to present some preliminary experimental data.

Background. For pressure oscillations without the presence of a radiant flux the classical linear QSHOD approximation results in the following expression for the pressure frequency response, R_p [1]:

$$R_p = \frac{\nu + \delta(\lambda - 1)}{1 + \left(r - \frac{k}{\lambda}\right)(\lambda - 1)}. \quad (1)$$

The parameters in this expression and below: f_r, fraction of q absorbed below surface reaction zone $J = \bar{q}/\rho\bar{r}_b C(T_s - T_0)$; $J^A = \bar{q}/\rho\bar{r}_b C\bar{T}_s - T_0^*)$; $k = (\bar{T}_s - T_0)(\partial \ln \bar{r}_b/\partial T_0)_{p,q=0}$; $k^* = (\bar{T}_s - T_0)(\partial \ln \bar{r}_b/\partial T_0)_{p,q}$; $k^A = (\bar{T}_s - T_0) \times (\partial \ln \bar{r}_b/\partial T_0^*)_p$; K_a, absorption coefficient; p, pressure; $q = (1 - r_\lambda)\tau_\lambda q_r$; q_r, external radiant flux; $r = (\partial \bar{T}_s/\partial T_0)_{p,q=0}$; $r^* = (\partial T_s/\partial T_0)_{p,q}$; $r^A = (\partial T_s/\partial T_0^*)_{p,q}$; r_b, burning rate; r_λ, reflectivity; $R_p = (\Delta r_b/\bar{r}_b)/(\Delta p/\bar{p})$; $R_q = (\Delta r_b/\bar{r}_b)/(\Delta q/\bar{q})$; T, temperature; $T_0^* = T_0 + \bar{q}/\rho\bar{r}_b C$; $TF = R_p/R_q$; X, length scale; $\beta_r = X_c/X_r(K_a\alpha_c/\bar{r}_b$; Δ, denotes an oscillatory variable; $\delta = \nu r - \mu k$; $\delta_q = \nu_q r^* - \mu_q k^*$; $\lambda = 1/2 + 1/2(1 + 4\Omega)^{1/2}$; $\mu = 1/(\bar{T}_s - T_0)(\partial \bar{T}_s/\partial \ln \bar{p})_{T_0,q=0}$; $\mu^* = 1/(\bar{T}_s - T_0)(\partial \bar{T}_s/\partial \ln \bar{p})_{T_0,q}$; $\mu_q = 1/(\bar{T}_s - T_0)(\partial \bar{T}_s/\partial \ln \bar{q})_{T_0,p}$; $\nu = (\partial \ln \bar{r}_b/\partial \ln \bar{p})_{T_0,q=0}$; $\nu_q = (\partial \ln \bar{r}_b/\partial \ln \bar{q})_{T_0,p}$; $\sigma_p = (\partial \ln \bar{r}_b/\partial T_0)_{p,q=0}$; $\sigma_p^* = (\partial \ln \bar{r}_b/\partial T_0)_{p,q}$; τ_λ — plume transmissivity; ω, angular frequency (rad/sec); $\Omega = \omega(\alpha_c/\bar{r}_b^2)$; superscripts and subscripts: *, $\bar{q} > 0$ included; c, convective = diffusive; 0, deep into the propellant ($x - -\infty$); r, radiant heat flux; R, reaction layer; s, surface; —, denotes the steady condition. The parameters are based solely on the steady burning characteristics, $\bar{r}_b(T_0, \bar{p})$ and $T_s(T_0, \bar{p})$. Equation (1) can also be cast in the «AB» form proposed by Culick [2].

Assuming $X_r \ll X_R$ (surface absorption) Zarko et al. [3] proposed a modification of two of the parameters in the QSHOD result for R_p to obtain an expression for the radiant heat flux frequency response, R_q. It was proposed that $\nu_q \equiv (\partial \ln \bar{r}_b/\partial \ln \bar{q})_{p,T_0}$ and $\delta_q = \nu_q r - \mu_q k$ replace ν and δ respectively, where $\mu_q \equiv [1/(\bar{T}_s - T_0)] (\partial \bar{T}_s/\partial \ln \bar{q})_{p,T_0}$. This is an extremely convenient form because if it is further assumed that $\delta_q = \delta = 0$, R_p is then related to R_q by the factor ν/ν_q at every frequency. Earlier, De Luca [4] proposed a similar relationship between R_q and R_p for surface absorption using a distributed FM approach. Since both these studies neglected the effect of the mean flux level this result is only valid if the k and r (or the A and B) parameters are not changed by the mean value of the radiant flux, along with the surface absorption assumption ($X_r \ll X_R$). Recently Son and Brewster [5] obtained a linear QSHOD expression for R_q using the ZN approach that includes in-depth absorption and the effect of the mean flux level. In the following section, this result is re-examined. A form of R_q as a function of the parameters originally proposed by Assovskii and Istratov [6] is also presented.

Generalized Expression

Applying the QSHOD assumptions, including Beer's law absorption, and solving the linearized energy equation results in the following expression [5]:

$$R_q = \frac{\nu_q + \delta_q(\lambda - 1) - \dfrac{k^* f_r J(\lambda - 1)}{\beta_r + \lambda - 1}}{1 + \left(r^* - \dfrac{k^*(\beta_r + \lambda - 1 + f_r J)}{\lambda(\beta_r + \lambda - 1)}\right)(\lambda - 1)}. \quad (2)$$

The mean flux level affects R_q explicitly through the dimensionless mean flux, J, and implicitly through changes in the k^* and r^* parameters (the * is used to indicate the presence of a radiant flux). In the general case of in-depth absorption the fom of Eqn. (2) is in a different form than Eqn. (1). However, for surface absorption the fraction of radiant flux absorbed below the surface zone, f_r, approaches zero and Eqn. (2) takes on the same form as Eqn. (1), but the implicit effect of the mean radiant flux can still potentially affect the values of the parameters. If the equivalence principle holds, ν_q and k^* are not independent parameters and it can be shown that $\nu_q = Jk^*$ so that ν_q can then be eliminated. Assuming further that the Jacobian term, δ_q, also vanishes (e. g., $\bar{r}_b = \bar{r}_b(\bar{T}_s)$), Eqn. (2) can be greatly simplified.

A similar expression can be obtained following similar steps by assuming at the start that the equivalence principle holds and defining the parameters as Assovskii and Istratov [6] have suggested (denoted with a superscript «A» here),

$$R_q = \frac{k^A J^A \left(1 - \dfrac{f_r(\lambda - 1)}{\beta_r + \lambda - 1}\right)}{1 + \left(r^A - \dfrac{k^A\big((\lambda - 1 - J)(\beta_r + \lambda - 1) + J^A f_r(\lambda - 1)\big)}{\lambda(\lambda - 1)(\beta_r + \lambda - 1)}\right)(\lambda - 1)}. \quad (3)$$

The zero frequency limit of Eqn. (3) is $R_q(\lambda \to 1) = k^A J^A/(1 + k^A J^A)$. The utility of this expression is that k^A and r^A may be easier to evaluate from known k and r data. Equation (3) can also be obtained by deriving relationships between k^*, r^*, J and k^A, r^A, and J^A and substituting these into the simplified version of Eqn. (2).

There is substantial interest in relating measurements of R_q to R_p. To accomplish this a transfer function is defined as $TF = R_p/R_q$. Performing the complex multiplication of TF with R_q will result in the desired R_p. Typically, the case of no external radiant flux, $J = 0$, is of interest for R_p. Therefore, from Eqns. (1) and (2) the most general form of the TF can be obtained. Assuming surface absorption ($f_r \to 0$), $\delta = \delta_q = 0$, and that $r^* = r$ and $k^* = k$ (approximately true for small mean radiant flux), the transfer function then becomes $TF = \nu/\nu_q$ so $|R_q|$ and $|R_p|$ are then simply related at every frequency by a single scaling factor and the phase shift would be the same for R_q and R_p. Further, if the equivalence principle holds, $TF = \nu/k^*J$. From these results, it is seen that ideally to obtain R_p from R_q measurements it is desirable to perform the experiments at the same pressure as the desired R_p ($k^* \sim k$, $r^* \sim r$), use a small mean radiant flux (if possible, such that $k^* \sim k$, $r^* \sim r$), and have a high absorption coefficient (if possible, such that $f_r \to 0$).

Linear Stability of Steady Burning

The linear stability of steady burning in the presence of a constant radiant flux is also of interest. Following similar steps as taken by Novozhilov [7] in the linear stability analysis of steady burning without an external radiant flux the linear stability can be obtained. For the case of surface absorption the stable burning regime has the same form as the case without an external radiant flux present, $r^* > (k^* - 1)^2/(k^* + 1)$, where again the values of k^* and r^* can in general be modified with the magnitude of the radiant flux. Kiskin [8] has previously performed the linear stability analysis using parameters as defined by Assovskii and Istratov [6] (assuming the equivalence principle holds and $\bar{r}_b = \bar{r}_b(T_s)$). The result reported by Kiskin for the opaque limit can also be obtained by substituting the following relationships into the above expression: $k^* = k^A(1 + J^A)/(1 + k^A J^A)$ and $r^* = r^A/(1 + k^A J^A)$. Including in-depth absorption in general results in a much more complex stability limit expression, but in the limit of a very translucent propellant ($X_r \gg X_c$) the following expression is obtained: $r^* > (k^* - 1)^2/[(1 - 2J)k^* + 1]$. These two limiting cases bracket the possible stability boundaries in the presence a constant radiant flux. Again, this result can be transformed into the form obtained by Kiskin for the same limiting case using the relationships above and $J^* = J^A/(1 + J^A)$.

Experimental Setup

A 100 W pulsed Nd:YAG (1.06 μm) laser was used as a radiant source. A Kistler 9207 microforce transducer was used to make the force measurements. Pneumatic vibration isolation was used to minimize the effect of extraneous vibrations. The laser beam was spatially integrated using a SPAWR beam integrator. The transmission loss through the plume above the burning propellant was measured with an embedded fiber optic. The fiber optic technique was also used to measure the spatial beam profile. The mean power was measured with an Ophir 1000 W power meter. A beam dump signal was monitored with a calibrated photodiode to obtain the time resolved radiant heat flux. Digital signal processing was used to analyze the data.

Experimental Results

Figures 1 and 2 show experimental results obtained using the radiant flux-recoil method using a propellant composed of AP (75 %, 11 μm), HTPB (24 %), and C (1 %, fine powder). Since the radiative source used can not be operated continuously, series of pulses were used to perturb the combustion. Two absorbed mean flux levels were considered: $\bar{q} = 2.3$ W/cm^2 and $\bar{q} = 11.4$ W/cm^2. The radiative losses due to optics, windows, the propellant plume transmission and reflection from the propellant have been accounted for. Figure 1 shows the ensemble averaged recoil response to various pulsings (all at 20.75 Hz). The mean recoil force and flux have been subtracted out. Several periods of pulsing (20—30 typically) have been averaged for each time trace. Two of the pulses shown were obtained at the lower mean power (2.3 W/cm^2) and one at the higher level (11.4 W/cm^2). The width of the pulse was varied for the low power case. The narrow pulse (roughly 1 ms wide) results in a large overshoot just after the end of the pulse that is likely a nonlinear effect. The wider pulse (roughly 3 ms wide) is composed of lower amplitude harmonics at high frequencies and therefore does not exhibit this type of overshoot. That is, the wide pulse case is likely exhibiting a more linear response than the narrow pulse case because the high frequency harmonics near the resonance peak frequency are lower in magnitude. The high power case (also roughly 3 ms wide) also does not exhibit the large overshoot. It can be seen that the oscillations for this case die out after a couple of cycles compared to the low power case that exhibits

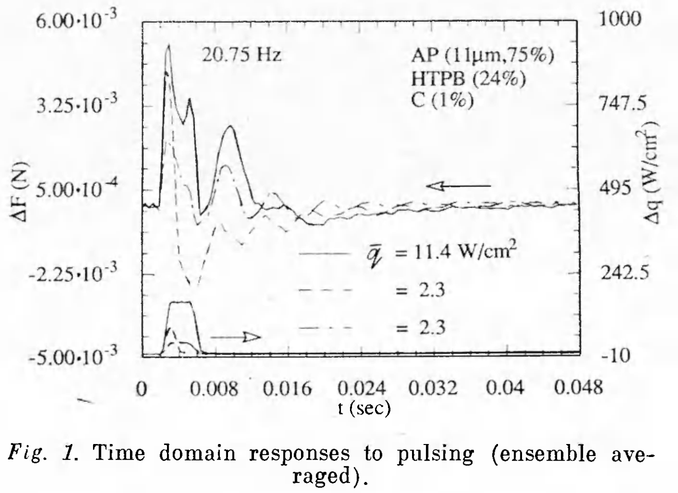

Fig. 1. Time domain responses to pulsing (ensemble averaged).

several periods of distinct oscillations even though the amplitude of the first oscillation after the pulse in the high power case is larger. In other words, the response of the higher power case appears more damped than the lower power case. These observations are likely due to the explicit and implicit mean heat flux effects on the radiant flux frequency response (see Eqn. (2)).

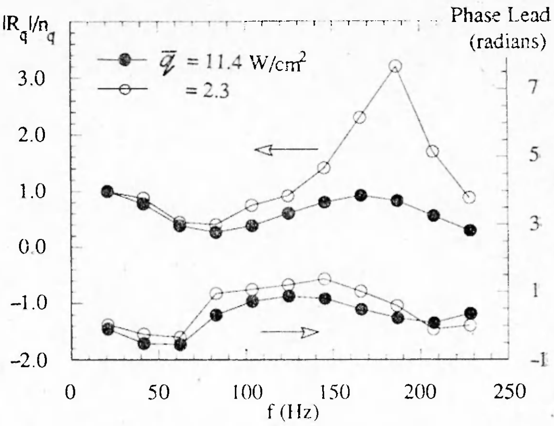

Fig. 2. Frequency domain responses.

The data was also digitally analyzed using a cross power spectral analysis. The magnitude of the recoil frequency response was normalized using the 20 Hz frequency value to obtain $|R_q|/n_q$. Signals with adequate signal-to-noise could be obtained up to about 230 Hz. Figure 2 shows the frequency response for the higher and lower radiant heat flux cases for the wider pulse (approximately 3 ms). At the lower frequencies the magnitude decreases a little and then at higher frequencies a distinct peak is evidenced. The first harmonics of the radiant flux have the largest amplitude, so the rise in the magnitude at lower frequencies may be evidence of small nonlinear effects on the measured response. The phase shift is close to zero at the lower frequencies rising to indicate the expected phase lead and then it approaches zero at the highest frequencies obtained in these tests. The main differences between the two cases are that the resonance peak in the magnitude appears to be flatter (more damped) and occurs at a lower frequency for the higher radiant flux level compared to the lower flux level. This comparison illustrates the effect of the mean flux level. This trend would be expected in propellants that exhibit a decrease in k^* with mean radiant flux level using Eqn. (2).

Summary

This paper has shown some recent results of a continuing theoretical and experimental investigation that is being conducted on radiant heat flux driven combustion of energetic materials. The radiant heat flux frequency response and linear stability, based on the ZN approach, is presented in terms of both k^*, r^* and J parameters, as well as k^A, r^A, J^A. Also, a method for obtaining the linear frequency response function over a range of frequencies from a single test using series of radiant pulses is demonstrated. Experimental results have been obtained for an AP/HTPB propellant that show a distinct effect of the mean flux. A high power (6 kW) CO_2 (10.6 μm wavelength) radiative source will shortly be used to obtain higher radiant fluxes and to obtain higher absorption coefficients since many materials are more opaque at wavelengths in the far infrared.

Acknowledgements

The support of the Office of Naval Research (N00014-91-J-1977), with R. S. Miller as contract monitor, is gratefully acknowledged.

REFERENCES

1. **Novozhilov B. V.** Burning of a powder under harmonically varying pressure // J. Appl. Mech. Tech. Phys.— 1965.— N 6.— P. 103—106.
2. **Culick F. E. C.** A review of calculations for unsteady burning of a solid propellant // AIAA J.— 1968.— 6(12).— P. 2241—2255.

3. **Zarko V. E., Simonenko V. N., Kiskin A. B.** Nonstationary combustion of condensed substances subjected to radiation // Combustion, Explosion, and Shock Waves.— 1987.— 23, N 5.— P. 16—26.
4. **De Luca L.** Frequency response function of burning solid propellants // Meccanica.— 1980.— P. 195—205.
5. **Son S. F., Brewster M. Q.** Linear burning rate dynamics of solids subjected to pressure or external radiant heat flux oscillations // AIAA J. Propulsion and Power, to appear 1993.
6. **Assovskii I. G., Istratov A. G.** Solid propellant combustion in the presence of light radiation // J. Appl. Mech. Tech. Phys.— 1971.— N 5.— P. 692—698.
7. **Novozhilov B. V.** Stability criterion for steady-state burning of powders // Ibid.— 1965.— N 4.— P. 157—160.
8. **Kiskin A. B.** Stability of stationary powder combustion acted on by a constant light flux // Combustion. Explosion, and Shock Waves.— 1983.— 19, N 3.— P. 295—297.

УДК 662.741.334

C. Zanotti and P. Giuliani

EXPERIMENTAL AND NUMERICAL APPROACH TO THE STUDY OF THE FREQUENCY RESPONSE OF SOLID PROPELLANTS

CNPM — National Research Council, Milan — ITALY

Abstract

The experimental study of the frequency response of burning solid propellants has been done using, as external forcing energy source, a CO_2 laser (60 W, 10.6 μm).

The laser radiant flux intensity was sinusoidally modulated and the response of the burning propellant was detected measuring the recoil force generated by the gases coming out from the burning surface using a strain-gage load cell which can operate inside the combustion chamber at the operating pressure. The tests were performed in the sub-atmospheric pressure range and a composite propellant (AP.HTPB/86.14) was used. The combustion chamber was filled by inert gas (N_2) and for each working pressure several tests were carried out at different radiant flux frequency modulations in the range from 5 to 50 Hz. The results evince that the recoil force amplitude depends on the forcing laser frequency with a maximum for every working pressure.

This experimental data set was then used to compare the nonlinear frequency response curves obtained by numerical integration of the combustion model equations. Comparisons between experimental and numerical results at 0.3 and 0.5 atm are shown and the general trend, obtained by numerical simulations, of the propellant frequency response vs pressure in a broader range is presented and discussed.

Introduction

The frequency response study of solid rocket propellants is a peculiar aspect related to the combustion instability problem in the motors. Many theoretical and experimental works were devoted to acquire more detailed knowledge of the phenomenon and many experimental techniques were developed to get data in a wide frequency range [1, 2].

The laser driven combustion technique is the method to influence the solid rocket propellant burning process which has advantages over others. The easiness to control and measure the transient, the possibility to choose different kind of waveforms and the contactless of the method make this equipment very flexible and convenient to be used.

This study, besides the importance to deepen the dynamic behavior of burning propellants, should give further information for the characterization of the composite propellant used in this work. In fact, it is experimentally well defined under steady state configuration [3], in the self-sustained oscillatory combustion regime close to the pressure deflagration limit [4, 5] and during the ignition transients [6—8]. The experimental work is mainly